Giant Modification of the Magnetocrystalline Anisotropy in Transition-Metal Monolayers by an External Electric Field

Kohji Nakamura,* Riki Shimabukuro, Yuji Fujiwara, Toru Akiyama, and Tomonori Ito
Department of Physics Engineering, Mie University, Tsu, Mie 514-8507, Japan

A. J. Freeman
Department of Physics and Astronomy, Northwestern University, Evanston, Illinois 60208, USA
(Received 7 October 2008; published 5 May 2009)

Controlling and designing quantum magnetic properties by an external electric field is a key challenge in modern magnetic physics. Here, from first principles, the effects of an external electric field on the magnetocrystalline anisotropy (MCA) in ferromagnetic transition-metal monolayers are demonstrated which show that the MCA in an Fe(001) monolayer [but not in Co(001) and Ni(001) monolayers] can be controlled by the electric field through a change in band structure, in which small components of the p orbitals near the Fermi level, which are coupled to the d states by the electric field, play a key role. This prediction obtained opens a way to control the MCA by the electric field and invites experiments.

DOI: 10.1103/PhysRevLett.102.187201 PACS numbers: 75.70.Ak, 71.20.Be, 73.20.At, 75.30.Gw

Magnetism of surface/interface structures and nanostructures continues to be one of the best-studied and important properties of materials with many exciting discoveries related to both fundamental and applied sciences [1,2]. One remaining key challenge lies in controlling and designing quantum magnetic properties with application of an external electric field, such as the use of magnetoelectric multiferroics that involve additional degrees of freedom introduced by utilizing both the charge and spin of electrons [3,4]. Very recently, the electric-field-induced modification of the magnetocrystalline anisotropy (MCA) in itinerant thin film ferromagnets has been demonstrated experimentally [5], in thin film FePt and FePd with liquid interfaces, where the coercivity is reversibly varied with application of a voltage. This effect is currently considered to be attributed to a change in the number of d electrons at the surface in response to the applied electric field. Further, the magnetization direction (i.e., the MCA) in the magnetic semiconductor (Ga, Mn)As within a metal-insulator-semiconductor structure has been successfully controlled by the application of an electric field [6]. Such exciting findings appear to be of great importance and to open a golden age of innovation in novel device physics.

Motivated by these experimental findings, we propose from first principles calculations an alternative mechanism for the change in the MCA in an itinerant thin film system by the external electric field. Indeed, we find that the MCA energy in an Fe(001) monolayer [but not in Co(001) and Ni(001) monolayers] is strongly modified (even its sign is changed) due to changes in the band structure introduced by the electric field, in which small components of the p orbitals near the Fermi level play a key role, which may lead to a giant MCA modification. The prediction obtained opens a way to control the MCA by the electric field and invites experiments.

As models, the simple systems of a freestanding Fe(001) monolayer with the lattice constant of 5.45 a.u. (Ag substrate), and Co(001) and Ni(001) monolayers with that of 4.83 a.u. (Cu substrate) are employed for investigating and understanding the electric field effect on the MCA, in which a symmetric geometry with a z reflection is set up. Calculations are performed by the full-potential linearized augmented plane wave (FLAPW) method [7–9] that treats film geometries, by including fully the additional vacuum regions outside of a single slab, where the wave functions are augmented by solutions of the one-dimensional (out-of-plane) Schrödinger equation and two-dimensional plane waves. Importantly, this single slab geometry, which is nonperiodic along the surface normal (z axis), allows a natural way to include the effect of an external electric field [10], compared to calculations that assume a superslab geometry (slabs separated by a vacuum region) in a bulk code [11,12].

The external electric field potential applied along the z axis, $v_{\mathrm{ext}} = F_{\mathrm{ext}} z$, is expanded into interstitial, MT sphere and vacuum regions, where F_{ext} and z are external electric field and z-axis position, respectively, and the quantization axis of the spherical harmonics is set along the z axis. Having a Hamiltonian with the added v_{ext}, self-consistent calculations are first performed in the scalar relativistic approximation (SRA), i.e., excluding the spin-orbit coupling (SOC), based on the local spin density approximation (LSDA) using the von Barth-Hedin exchange-correlation [13]. Although many-body effects beyond the LDA might be of importance in electric field problem [14], results obtained within LDA in metallic systems, as done previously [10,11], may be sufficient to discuss conclusions. LAPW functions with a cutoff of $|\mathbf{k} + \mathbf{G}| \leq 3.6$ a.u. are used, where the angular momentum expansion inside the MT sphere is truncated at

TABLE I. Calculated spin and orbital moments, m_{001}^{spin} and m_{001}^{orbit} (in μ_B), in the MT spheres when the magnetization is oriented along the [001] directions, the anisotropy of moments, $\Delta m = m_{001}$-m_{100}, and MCA energy, E_{MCA} (in meV/atom), for Fe(001), Co(001), and Ni(001) monolayers. FT and SC represent force theorem and self-consistent ways for treating the spin-orbit coupling.

System	Method	Zero field					$F_{\text{ext}} = 1$ eV/Å				
		m_{001}^{spin}	Δm^{spin}	m_{001}^{orbit}	Δm^{orbit}	E_{MCA}	m_{001}^{spin}	Δm^{spin}	m_{001}^{orbit}	Δm^{orbit}	E_{MCA}
Fe	FT	3.163	0.000	0.155	−0.002	0.19	3.163	0.001	0.158	−0.014	0.02
	SC	3.162	0.000	0.155	−0.002	0.22	3.163	0.000	0.158	−0.014	0.06
Co	FT	2.085	−0.001	0.144	−0.099	−1.37	2.085	−0.001	0.144	−0.099	−1.39
	SC	2.084	−0.001	0.144	−0.099	−1.37	2.084	−0.001	0.144	−0.099	−1.37
Ni	FT	0.987	−0.002	0.125	−0.101	−1.70	0.987	−0.002	0.125	−0.100	−1.69
	SC	0.985	−0.002	0.124	−0.100	−1.68	0.985	−0.002	0.125	−0.100	−1.67

$\ell = 8$ for wave functions, charge and spin density and potential.

To determine the MCA, first the second variational method [15,16] for treating the SOC is performed by using the calculated eigenvectors in the SRA, and the MCA energy E_{MCA} is determined by the force theorem [17,18], which is defined as the energy eigenvalue difference for the magnetization oriented along the in-plane [100] and out-of-plane [001] directions. With 7056 special **k** points in the two-dimensional Brillouin zone (BZ), the E_{MCA} was found to sufficiently suppress numerical fluctuations. Table I summarizes the spin and orbital moments and the E_{MCA} calculated in an electric field of zero and 1 eV/Å for the Fe(001), Co(001), and Ni(001) monolayers. To confirm the validity of the force theorem, total energy self-consistent calculations including the SOC are also carried out, and those results are also given in Table I. Values of the spin and orbital moments and the E_{MCA} in the force theorem are found to be almost identical to those from the self-consistent calculations—which confirms the validity of applications of the force theorem [17] even for the systems in an electric field.

For the Fe(001) monolayer, the E_{MCA} in zero field has a positive value of 0.19 meV/atom (in FT) and 0.22 meV/atom (in SC), indicating that the magnetization energetically favors pointing in the out-of-plane [001] direction. When the electric field is introduced, the E_{MCA} significantly decreases as F_{ext} increases and becomes even negative as F_{ext} becomes larger than about 1 eV/Å, as shown in Fig. 1. We also find that, although the spin moments are almost identical over a range of applied electric field, the orbital moments in the in-plane [100] direction are strongly enhanced due to the electric field. Interestingly, in contrast, for the Co(001) and Ni(001) monolayers, the E_{MCA} as well as the orbital moments do not change with application of the electric field.

Next, within a rigid band model, we analyzed the behavior of the MCA energy with respect to an assumed variation of the number of valence electrons, N. The results are shown in Fig. 2 for the Fe(001) and Co(001) monolayers. For Fe(001), E_{MCA} in zero field decreases as N increases, where the E_{MCA} has positive values for N less than about 8.1 and negative values for more than about 8.1. The slope, $dE_{\text{MCA}}/dN = -2.6$, at $N = 8$, which corresponds to the number of valence electrons in the Fe system, indicates that an increase (decrease) of 0.01 electrons depresses (enhances) the E_{MCA} by 14%. In the case of the Co(001) monolayer, the slope results in a small positive value of 1.1 at $N = 9$. Note that a scenario based on the change in the number of valence electrons is ruled out in explaining the MCA modification. When the electric field is introduced, the behavior of the MCA with the number of valence electrons is qualitatively identical to that in zero field, but the modification in the MCA for the Fe system clearly appears and strongly depends on the number of valence electrons. A maximum increment (and change of sign) of the E_{MCA} is achieved at $N \approx 8.4$.

In order to clarify the origin of the MCA modification, the Fe(001) band structures and the MCA energy contribution, [19] $E_{\text{MCA}}(\mathbf{k})$, are calculated, and shown in Fig. 3. In zero field, the bands crossing the Fermi level (E_F) arise mainly from the minority-spin states, while the majority-spin bands (not shown in the figure) are almost fully occupied and are located from −1 to −4 eV below E_F. In the minority-spin states, bands 3 ($d_{x^2-y^2}$) and 4 (d_{xy}) located above and below E_F, and whose orbitals lie in the layer plane, show a large dispersion due to the strong bonding between them; band 1, whose d_{z^2} orbital lies along the plane normal and shows a weak dispersion, is

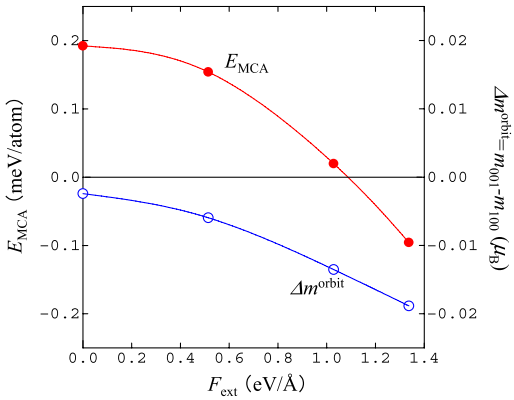

FIG. 1 (color online). Calculated MCA energy, E_{MCA}, and the anisotropy of orbital moments, $\Delta m^{\text{orbit}} = m_{001}$-$m_{100}$, as a function of the external electric field, F_{ext}, for the Fe(001) monolayer.

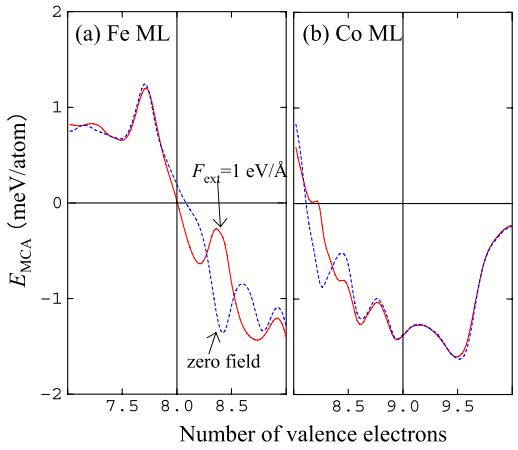

FIG. 2 (color online). Calculated MCA energy, E_{MCA}, as a function of the number of valence electrons, N, for the Fe(001) and Co(001) monolayers. Dashed and solid lines represent results for an external electric field of zero and 1 eV/Å values, respectively. The point at $N = 8$ (9) corresponds to the number of valence electrons in the present Fe (Co) system.

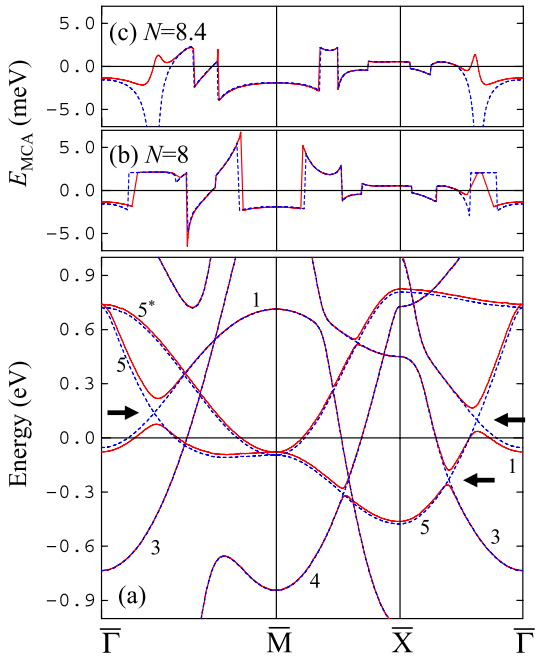

FIG. 3 (color online). (a) Calculated minority-spin band structure along high-symmetry directions for an Fe(001) monolayer in an external electric field of zero (dotted lines) and 1 eV/Å (solid lines). The reference energy ($E = 0$) places the Fermi energy, E_F. Arrows indicate band gaps induced by the electric field. Bands 1, 3, and 4 stand for d_{z^2}, $d_{x^2-y^2}$, and d_{xy} states, respectively, and bands 5 and 5* are weakly bonding and antibonding $d_{xz,yz}$ states. (b) MCA energy contribution, $E_{MCA}(\mathbf{k})$ [19] in zero field (dotted line) and at 1 eV/Å (solid line). (c) Results when the number of valence electrons, N, is set to 8.4 within the rigid band.

located above E_F except near $\bar{\Gamma}$; bands 5 and 5* ($d_{xz,yz}$) with weakly bonding and antibonding states are seen to cross E_F.

As pointed out previously [15,20], in this band structure, the MCA originates mainly from the SOC between the minority-spin bands crossing E_F. According to perturbation theory [20], the SOC between occupied and unoccupied states with the same (different) m magnetic quantum number through the L_z (L_x and L_y) operator gives a positive (negative) contribution to the $E_{MCA}(\mathbf{k})$. As seen in Fig. 3, at around $\bar{\Gamma}$, the SOC interaction between the occupied d_{z^2} ($m = 0$) state at -0.05 eV and the unoccupied $d_{xz,yz}$ ($m = \pm 1$) state at 0.7 eV yields a negative $E_{MCA}(\mathbf{k})$. Around $\bar{M}$, the SOC interaction between the occupied $d_{xz,yz}$ state at -0.1 eV and the unoccupied d_{z^2} state at 0.7 eV also makes for a negative $E_{MCA}(\mathbf{k})$. However, in most of the BZ except around $\bar{\Gamma}$ and $\bar{M}$, the contribution is mostly positive from the SOC between the occupied and unoccupied $d_{xz,yz}$ states.

When the electric field is introduced, although the overall band structure is similar compared to that in zero field, a significant difference is observed near regions indicated by arrows in Fig. 3, e.g., two intersecting bands 1 and 5 above E_F at $\frac{1}{3}(\bar{\Gamma}$-$\bar{M})$ hybridize with each other and are split by about 0.2 eV. Around $\frac{3}{5}(\bar{X}$-$\bar{\Gamma})$, the lowered band is almost pushed down below E_F by the electric field.

The electric field, which breaks the z-reflection symmetry, promotes a variety of new electronic structures such as a lifting of degenerate energy states. Importantly, the electric field potential in the MT spheres, which is described with the Y_0^1 spherical harmonic, allows an interaction between two states with angular quantum numbers of ℓ and $\ell \pm 1$ (e.g., p and d orbitals) and the same magnetic quantum number m, since the field matrix $\langle \ell' m' | Y_0^1 | \ell m \rangle$ is nonzero when $\ell' = \ell + 1$ and $m' = m$. Indeed, small components of the p orbitals are found to appear in the bands near E_F, as indicated by circles (p_z) and triangles ($p_{x,y}$) in Fig. 4. Thus, the p_z ($m = 0$) orbitals in band 5 above E_F at $\frac{1}{3}(\bar{\Gamma}$-$\bar{M})$ couple to the d_{z^2} states of band 1, and so these

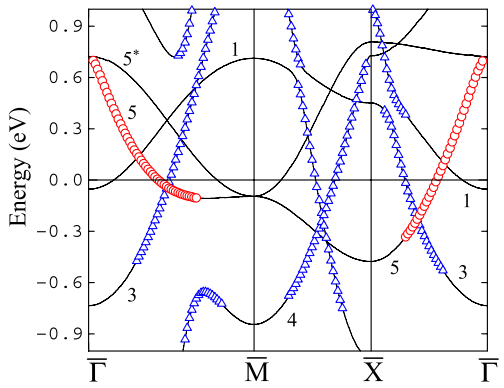

FIG. 4 (color online). Calculated band structure in zero field along high-symmetry directions for an Fe(001) monolayer. Open circles and triangles represent bands having small components (possessing more than 1% in the Fe muffin-tin sphere) of p_z and $p_{x,y}$ orbitals, respectively.

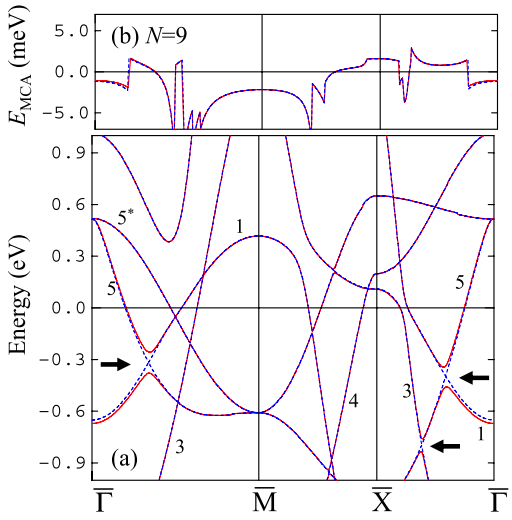

FIG. 5 (color online). Calculated minority-spin band structure and MCA energy contribution, $E_{\mathrm{MCA}}(\mathbf{k})$ [19], along high-symmetry directions for a Co(001) monolayer in an external electric field of zero (dotted lines) and 1 eV/Å(solid lines). Notation, the same as in Fig. 3.

bands are split. Also, the $p_{x,y}$ ($m = \pm 1$) orbitals in band 3 below E_F at $\frac{1}{3}(\bar{X}\text{-}\bar{\Gamma})$ couple to the $d_{xz,yz}$ states of band 5; the p_z orbitals in band 5 above E_F at $\frac{3}{5}(\bar{X}\text{-}\bar{\Gamma})$ couple to the d_{z^2} states of band 1 as well. The induced energy band gaps are found to increase as F_{ext} increases. Such an F_{ext} dependence may justify our proposed mechanism of the MCA change even in nonsymmetric slab systems without z reflection. Thus, small components of the p orbitals play a key role in determining the band structure when the electric field is introduced.

Although the trend in $E_{\mathrm{MCA}}(\mathbf{k})$ in the electric field is almost identical compared to that in zero field, as seen in Fig. 3(b), in the vicinity around $\frac{1}{3}(\bar{\Gamma}\text{-}\bar{M})$ the band gap induced by the electric filed enlarges a region of negative $E_{\mathrm{MCA}}(\mathbf{k})$. Around $\frac{3}{5}(\bar{X}\text{-}\bar{\Gamma})$, the positive contribution to $E_{\mathrm{MCA}}(\mathbf{k})$ in zero field becomes negative, where the induced band gap near E_F gives rise to the negative contribution from the SOC interaction between the d_{z^2} and $d_{xz,yz}$ states. In addition, when N is chosen to be 8.4 within the rigid band, which corresponds to E_F of about 0.12 eV, the large MCA modification can be confirmed to be related to the induced band gaps around $\frac{1}{3}(\bar{\Gamma}\text{-}\bar{M})$ and $\frac{3}{5}(\bar{X}\text{-}\bar{\Gamma})$ [see Figs. 2 and 3]. Moreover, for the Co(001) monolayer, E_F further shifts above the d bands due to an increase in the number of electrons as seen in Fig. 5, and so the states around the induced band gaps become occupied. Hence, no change in the MCA appears in the Co system (also in the Ni one) as mentioned.

In summary, we investigated the effects of the external electric field on the MCA energy in transition-metal monolayers by means of the first principles FLAPW method, and found that the MCA energy in the Fe(001) monolayer [but not in the Co(001) and Ni(001) cases] can be modified through changes in the band structure, in which small components of the p orbitals near E_F, which are coupled to the d states due to the presence of the electric field, play a key role. The predicted results open a way to control the MCA by an external electric field and invites experimental confirmation for systems such as an Fe thin film sandwiched by insulators such as MgO. Indeed, very recently, an experimental intimation for the MCA change in an ultrathin Fe/MgO junction was reported [21].

We thank Jung-Hwan Song for fruitful discussions and suggestions. Work at Mie University was supported by a Grant-in-Aid for Scientific Research (No. 20540334), and for computations performed at ISSP, University of Tokyo. Work at Northwestern University was supported by the U.S. Department of Energy (DE0FG02-88ER 45372).

*kohji@phen.mie-u.ac.jp

[1] A. J. Freeman and R. Q. Wu, J. Magn. Magn. Mater. **100**, 497 (1991), and references therein.
[2] S. D. Bader, Rev. Mod. Phys. **78**, 1 (2006), and references therein.
[3] W. Eerenstein *et al.*, Nature (London) **442**, 759 (2006), and references therein.
[4] R. Rames and N. A. Spaldin, Nature Mater. **6**, 21 (2007), and references therein.
[5] M. Weisheit *et al.*, Science **315**, 349 (2007).
[6] D. Chiba *et al.*, Nature (London) **455**, 515 (2008).
[7] E. Wimmer *et al.*, Phys. Rev. B **24**, 864 (1981).
[8] M. Weinert, E. Wimmer, and A. J. Freeman, Phys. Rev. B **26**, 4571 (1982).
[9] K. Nakamura *et al.*, Phys. Rev. B **67**, 014420 (2003).
[10] W. Weinert *et al.*, J. Phys. Condens. Matter **21**, 084201 (2009).
[11] J. Neugebauer and M. Scheffler, Phys. Rev. B **46**, 16067 (1992).
[12] B. Meyer and D. Vanderbilt, Phys. Rev. B **63**, 205426 (2001).
[13] U. von Barth and L. Hedin, J. Phys. C **5**, 1629 (1972).
[14] X. Gonze, P. Ghosez, and R. W. Godby, Phys. Rev. Lett. **74**, 4035 (1995).
[15] R. Wu and A. J. Freeman, J. Magn. Magn. Mater. **200**, 498 (1999).
[16] C. Li *et al.*, Phys. Rev. B **42**, 5433 (1990).
[17] G. H. O. Daalderop, P. J. Kelly, and M. F. H. Schuurmans, Phys. Rev. B **41**, 11 919 (1990).
[18] X. D. Wang *et al.*, J. Magn. Magn. Mater. **159**, 337 (1996).
[19] Since the introduction of an external electric field and SOC breaks the lattice symmetry in the system, the E_{MCA} in Figs. 3 and 5 is averaged for the magnetizations oriented along the ⟨100⟩ and ⟨010⟩ directions.
[20] D. S. Wang, R. Wu, and A. J. Freeman, Phys. Rev. B **47**, 14 932 (1993).
[21] T. Maruyama *et al.*, in *Proceedings of the 53rd Annual Conference on Magnetism and Magnetic Materials* (Report No. BD-01, 2008); Nature Nanotech. **4**, 158 (2009).